

Title:

Updating Nonlinear Finite Element Models in the Time Domain

Author(s):

Paula J. Beardsley, Francois M. Hemez,
and Scott W. Doebling

Submitted to:

<http://lib-www.lanl.gov/la-pubs/00538367.pdf>

Updating Nonlinear Finite Element Models in the Time Domain

Paula J. Beardsley, Francois M. Hemez, and Scott W. Doebling

Engineering Analysis Group
Los Alamos National Laboratory
Los Alamos, New Mexico, USA

ABSTRACT

This paper describes the implementation, verification, and comparison of two techniques for updating nonlinear finite-element structural dynamics models using transient time-domain data. The methods are motivated in terms of the intended applications, and the derivations are shown as they relate to the model updating methods for linear finite element models. The application of the two methods to simulated results for an impact problem (with a structure containing a hyperelastic polymer) is presented.

SECTION 1. INTRODUCTION

In many engineering applications it is advantageous or necessary to possess an accurate means of predicting the dynamic response of a system. Many of these systems contain significant geometric complexity or nonlinearity causing acquisition of an analytical representation to be impossible. Because of this, the finite element method (FEM) is often used in the modeling of such systems. While being a powerful tool, the FEM is inherently based on approximation leading to a direct contradiction with the goal of having an accurate device for response prediction. One approach taken to remedy this contradiction is to use measurement data taken from the modeled system to update the finite element model, so improving its predictive quality. Adapting this approach for use with nonlinear systems and applying it to a simple nonlinear test structure has been the focus of this research.

Development of methods of finite element updating for nonlinear systems could have a significant effect on the manner in which structural health monitoring is

carried out. These methods would be particularly influential in the area of damage identification. Model updating can be used to gain a more accurate prediction of the response for an undamaged structure. The possession of an accurate model facilitates simpler recognition of the presence of damage. The updating procedure would also be applicable for locating and quantifying any structural damage. This technique could serve as an replacement for traditional, labor-intensive methods of damage detection.

In this paper, the methods are applied to characterize the stress-strain curve of a hyperelastic polymer foam. The experiment described in this paper is designed to be a geometrically simple yet nonlinear precursor to the eventual application of this technology. The eventual goal is to update a large finite element model with multiple metal/metal and metal/polymer interfaces using data from a corresponding experimental structure subjected to explosive shock loads. Another possible application of this technology that will eventually be explored is the characterization of strain-rate-dependence in the constitutive models of polymeric materials, such as the foam layer described in this paper. This technique has the potential to cover strain-rate ranges not coverable by current techniques (e.g. Split Hopkinson Bar).

Here is an outline of the paper: **SECTION 1** introduces the research by providing motivation and potential applications. A brief explanation of the challenges of nonlinear updating is presented in **SECTION 2** in the form of a comparison with linear updating methods. **SECTION 3** is devoted to a description of an experiment designed to verify the nonlinear updating techniques of **SECTION 2** and results of experimental simulation and updating are given. Finally, a summary of the conclusions and future work for this project is contained in **SECTION 4**.

SECTION 2. NONLINEAR FINITE ELEMENT MODEL UPDATING

This section provides a description of the steps involved in updating a nonlinear FEM while highlighting the difficulties that arise when analyzing nonlinear rather than linear systems. The initial step naturally includes the development of a finite element model of the system's dynamics. It is important that the model to be updated be a reasonably accurate approximation of the real system. A FE model that produces a response drastically different from the measurement data is unlikely to converge upon updating. For linear systems, the dynamic equation of motion can be expressed as

$$[M(p)]\{a(t)\} + [K(p)]\{u(t)\} = \{Fe(t)\} \quad (1)$$

which is representative of the equilibrium between inertial forces, internal (linear) forces and applied loading. This equation clearly denotes the dependency of the mass and stiffness matrices on the model parameters $\{p\}$ and expresses the parametric nature of FE models. It is these parameters that are updated to increase the correlation between the measured and finite element model data.

Since the dynamics are linear, equation (1) can be transformed to the frequency domain using a convolution operator. The resulting equation relates the input and

output frequency response functions (FRF) of the system at any given sampling frequency λ as

$$[K(p) - \lambda[M(p)]]\{u(\lambda)\} = \{Fe(\lambda)\} \quad (2)$$

Consideration of the homogenous version of equation (2) nets the system resonant frequencies, λ , and mode shapes, $\{\phi\}$, which, upon the addition of orthogonality conditions, provide a basis for the subspace to which the response, $\{u(\lambda)\}$, belongs.

The dynamic equation of motion for nonlinear systems is simply equation (1) modified by the addition of the nonlinear internal force vector, $\{Fi(p, t)\}$, as shown in equation (3),

$$[M(p)]\{a(t)\} + [K(p)]\{u(t)\} + \{Fi(p, t)\} = \{Fe(t)\} \quad (3)$$

The addition of the nonlinear force term changes the interpretation of the system's behavior in the frequency domain because signals resulting from this system are no longer necessarily periodic. This being the case, meaningful dynamic response analyses must be completed in the time domain.

The basis of finite element model updating is the correlation of FE model simulated data with measurement data and the minimization of the difference. One way to quantify this difference is to define residue vectors and incorporate them into the system's dynamic equation of motion. For linear systems, the frequency domain based equilibrium expression, equation (2), is often used during correlation. Experimentally, the system's modal quantities, $\{\phi_{test}\}$ and λ_{test} , are determined from measured FRFs or directly from time-domain data using identification algorithms [1]. These modal quantities, when substituted into the finite element model dynamic equation of motion, result in a violation of equilibrium that can be corrected by the incorporation of residue vectors:

$$[K(p)]\{\phi_{test}\} = \lambda_{test} [M(p)]\{\phi_{test}\} + \{Rf(p, \lambda)\} \quad (4)$$

Here, the modal residue vectors, $\{Rf(p, \lambda)\}$, account for the out-of-balance forces in the model. Vectors $\{Rf(p, \lambda)\}$ contain the largest entries at the degrees of freedom where the equilibrium is violated the most. This can be used as the basis for: 1) Identifying the source of modeling error; and 2) Updating the model by minimizing a norm of vectors $\{Rf(p, \lambda)\}$. This approach is referred to as force-based model updating since entries of residues $\{Rf(p, \lambda)\}$ in equation (4) are consistent with forces.

The objective function, which is the quantity that when minimized results in correlation between the test and finite element model data, can be defined as the norm of the residue vectors. This is shown in equation (5).

$$J(p) = \|Rf(p, \lambda)\| \quad (5)$$

For simplicity, we assume that time-domain, displacement measurements $\{u_{test}\}$ are obtained by instrumenting the system. However, it can be verified easily that all developments below apply to arbitrary combinations of displacement, velocity and

acceleration measurements. (Note that higher-order derivatives such as strains could also be employed.)

As mentioned previously, nonlinear systems generally do not allow for much meaningful interpretation in the frequency domain. This being the case, correlation between finite element model and measurement data must be done in the time domain. Here we present two different implementations for solving the nonlinear inverse problem. The first approach is the rather obvious definition of the residue vectors as the difference between the test and simulation data, as shown in equation (6). The objective function to be minimized, $J(p)$, is defined as the 2-norm of these residue vectors: note that the same definition applies in the linear case with modal residues (4).

$$\{R(p, t)\} = \{u_{test}(t)\} - \{u(t)\} \quad (6)$$

$$J(p) = \|R(p, t)\| \quad (7)$$

The correlation approach presented above can be viewed as a rather conventional generalized least-squares (GLS) minimization. The GLS formulation has been used for solving inverse problems in many engineering applications for several decades. It is well known that its success is conditioned by the ability of the math model to span the subspace to which the test data belongs. It is interesting to notice that this is exactly what modal correlation attempts with linear systems since the measured response belongs to a subspace spanned by the identified mode shapes.

Along these lines, the principal component decomposition (PCD) method, developed and validated in Reference [2], attempts to generalize the notion of a “mode shape” for nonlinear systems. Rather than using the direct comparison of expression (6), the singular value decomposition (SVD) of time-domain data is first performed to get equation (8). Residue vectors (9), (10), and (11) can be extracted from this.

$$[U][\Sigma][V(t)]^T = SVD([u(t)]) \quad (8)$$

$$[R_U(p, t)] = [U_{test}]^T [U] - I \quad (9)$$

$$[R_\Sigma(p, t)] = [\Sigma_{test}] - [\Sigma] \quad (10)$$

$$[R_V(p, t)] = [V_{test}(t)]^T [V(t)] - I \quad (11)$$

In the above, U_{test} , Σ_{test} , and $V_{test}(t)$ refer to the principal components extracted from the measured data; U , Σ , and $V(t)$ refer to the principal components extracted from the finite element model simulated data; and I is the identity matrix. Because the singular vectors are orthogonal, they provide a basis of the multi-dimensional space to which the nonlinear signals belong [3]. The PCD approach consists of minimizing the distance between these decompositions rather than between the original signals. The objective function to be minimized is defined as the sum of the norms of these residues,

$$J(p) = W_U \|R_U(p, t)\| + W_\Sigma \|R_\Sigma(p, t)\| + W_V \|R_V(p, t)\| \quad (12)$$

The final step in the finite element model updating process is the generation of the model's response surface, which is essentially a look-up table containing the chosen objective function, $J(p)$, evaluated at a range of model parameters, $\{p\}$. The key to building the response surface is the selection of values for the model parameters. A large enough number of values must be used to completely define the surface or the correct minimum may not be located. In opposition to this, a large number of values will result in large numbers of finite element analyses and escalating CPU costs.

The objective function was defined such that minimization would result in the best correlation between the simulated and measured data sets. This being the case, once the response surface has been constructed, updating the model is reduced to the task of finding the smallest value on the response surface. The parameter values that correspond to this smallest value are those that should be used to update the model.

SECTION 3. EXPERIMENTAL VERIFICATION

In order to verify the effectiveness of the nonlinear finite element model updating techniques discussed in **SECTION 2**, a simple experiment was designed to incorporate nonlinearity from multiple sources. The experimental structure consists of a cylindrical steel impactor and a foam (cushion) layer assembled on a mounting plate and attached to a drop table. This assembly is illustrated schematically in **FIGURE 1**.

During the experiment the table is dropped from a height to produce a velocity of 500 in/sec at impact. Accelerometers are placed on top of the steel to collect measurement data that can be used for validating the predictive quality of our models. At press time, the experiment was still being developed. As a preliminary step to using measurement data from the drop test to update the finite element model, simulated experimental data was generated as a substitute. This section describes the experiment and the results of updating the finite element model using simulated experimental data.

A description of the geometric configuration used for this experiment is given here. The steel and foam cylinders have the following dimensions:

Outer radius:	3.000 inches
Inner radius:	0.250 inches
Thickness of steel:	3.000 inches
Thickness of foam:	0.375 inches

Both cylinders have hollowed centers and have been fixed with a rigid collar to restrict the motion of the impactor to the vertical direction.

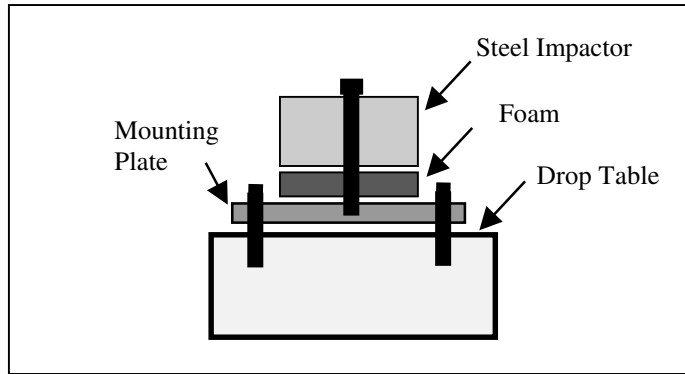


FIGURE 1. Schematic of Steel/Foam Impact Experiment

This experiment was designed to incorporate nonlinearity from both the impact conditions and the foam material behavior. The foam layer is a hyper-elastic material that is highly compressible. It has the following properties:

Density: $2.744\text{e-}04 \text{ lbf/in}^3$

Poisson's Ratio: 0.0

The stress-strain properties of this material are defined using pseudo-static uniaxial test data. FIGURE 2 shows this data plotted along with a parabolic curve fit to the data. It can be observed from this figure that the foam behavior is fairly linear up to 15% deformation. However, for deformations higher than 15%, the material's nonlinearity is clearly visible.

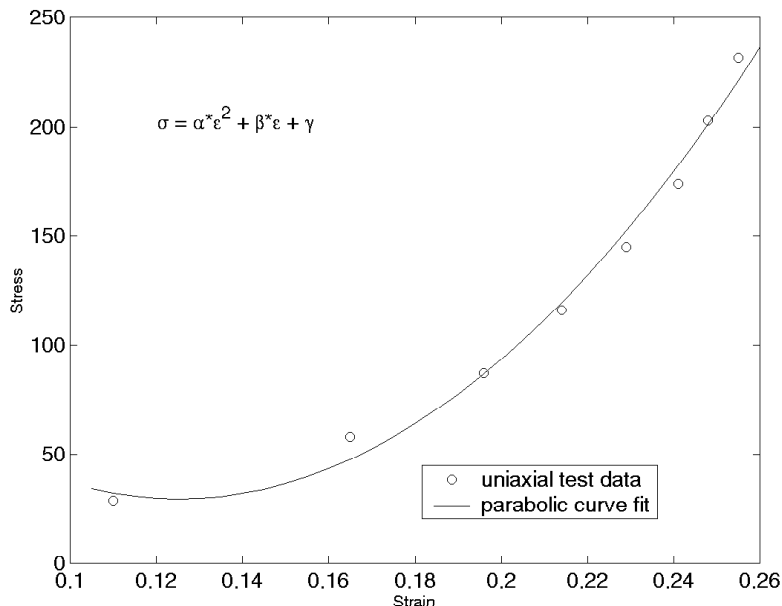


FIGURE 2. Uniaxial Test Data for Foam Material and Parabolic Curve Fit

The steel material demonstrates only its elastic behavior during this experiment, thus nonlinearity does not enter the experiment from this source. The elastic behavior of the steel (SS304, stainless steel) is described by the following properties:

Density:	7.41e-04 <i>lbf / in</i> ³
Modulus of Elasticity	28.7e+06 psi
Poisson's Ratio:	0.264

Geometric, material, and operational specifications for the drop table are given in Reference [3].

The finite element model of this experimental system was developed using the HKS ABAQUS/Explicit, a general-purpose package for finite element modeling of nonlinear structural dynamics [4]. It features an explicit time integration algorithm, which is convenient when dealing with nonlinear material behavior, potential sources of impact, and high frequency excitations.

In order to create the response surface, it was first necessary to determine which model parameters were variable and not well known and therefore good candidates for updating. The impact velocity, which can be approximately determined from the drop height, was chosen as an updating parameter. The foam material model, which was defined by uniaxial stress-strain data, is somewhat uncertain because little information is known about the behavior of the foam at high strain rates. As a result of this, a parameter representative of the foam's material behavior was chosen for updating. This parameter, referred to as alpha in this paper, is the coefficient of the highest order term from the parabolic curve fit to the stress strain data of the foam. FIGURE 2 shows the result of the parabolic curve fit. The limit states and analysis points for both model parameters to be updated were selected and are listed in TABLES I and II.

TABLE I. Magnitude of Alpha Perturbations

% nominal	Alpha
95.0	1.0804e+04
97.5	1.1089e+04
100.0	1.1373e+04
102.5	1.1657e+04
105.0	1.1942e+04

TABLE II. Magnitude of Impact Velocity Perturbations

% nominal	Velocity (in/sec)
82.0	410
88.0	440
94.0	470
100.0	500
106.0	530
112.0	560
118.0	590

The choice of the parameter variations listed in TABLES I and II result in a total of 35 finite element analyses that need to be completed to build the response surface. Completing this number of analyses is feasible because of the simplicity of the model. From each analysis, the acceleration history at three evenly spaced points around the top of the steel cylinder was recorded.

Building the response surface required the evaluation of the objective functions for each of the parameter variations. For this experiment, two objective functions, equations (7) and (12), were used, substituting acceleration data for displacements, to build two separate response surfaces. These objective functions are a measure of difference between the response generated at each model parameter perturbation point and the response of the simulated experiment. In generating the simulated experimental data, the values listed in TABLE III under Experiment were chosen. The response surfaces generated using the GLS and PCD objective functions are shown in FIGURE 3. It should be noted that for a certain range of the updating parameters, the solution of the impact problem did not converge properly, resulting in the large “peak” that is evident in FIGURE 3(a). Also, during the update process the minimum value of the objective function was linearly interpolated between the evaluated points in TABLES I & II.

Finding the minimum point on each of these response surfaces produced the updated parameters listed in TABLE III, from which it is clear that both objective functions produced the correct impact velocity. The values obtained for alpha from the response surface varied from the actual value by up to 0.6%. The minimum point on the response surface did not correspond exactly with the experimental model because a finite element analysis was not evaluated at that point. Using these updated parameter values the acceleration histories shown in FIGURE 4 were produced. This figure shows very close correlation between the experimental acceleration data and the acceleration data obtained from both updated finite element models and significant improvement over the nominal model.

TABLE III. Nominal, Experimental, and Updated Model Parameters

Parameter	Nominal	Experiment	GLS Updated	PCD Updated
Alpha	11000	11600	11666	11654
Velocity	500.00	500.00	499.09	500.90

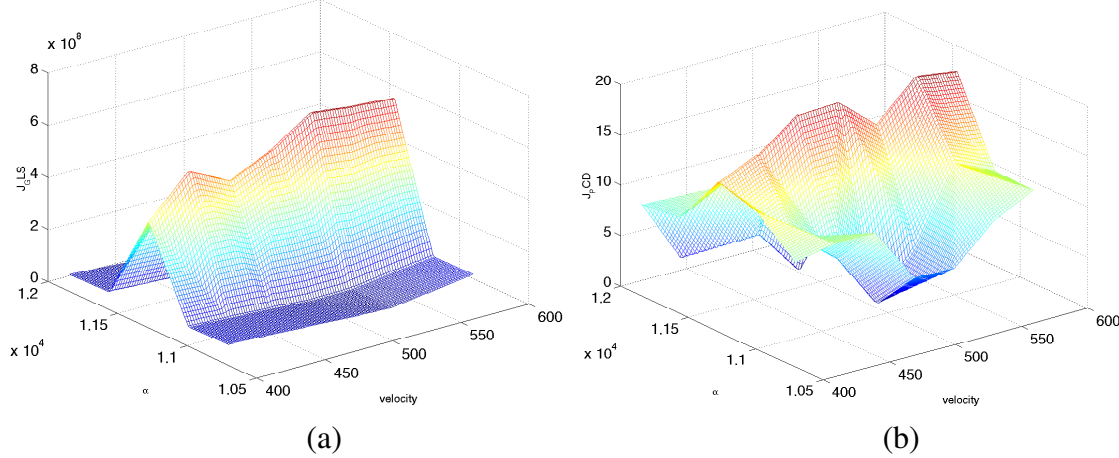


FIGURE 3. Response Surfaces Generated Using (a) GLS and (b) PCD Objective Functions

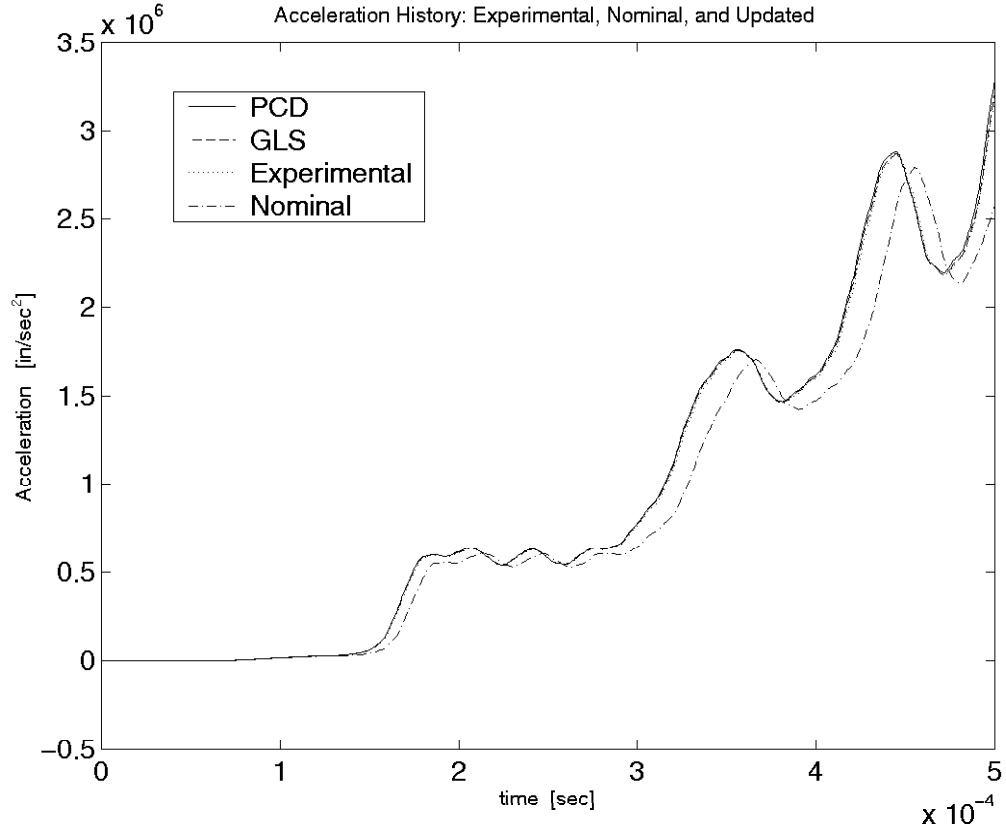


FIGURE 4. Acceleration Histories of Simulated Experiment and Updated Models

Section 4. Comments and Conclusions

The results displayed in **SECTION 3** allow the following observations to be made. Although both methods successfully updated the model producing acceleration responses that were almost indistinguishable from those of the experiment, a more refined response surface mesh (that is, more finite element analyses) would likely have produced improved results. No pronounced difference in effectiveness was noticeable between the two approaches. However, the GLS response surface in **FIGURE 3(a)** shows a decreased sensitivity to changes in the velocity parameter, which could cause numerical problems during the optimization and lead to an undetermined solution. The many peaks and valleys visible in the PCD response surface in **FIGURE 3(b)** make it unlikely that these same problems would occur. The GLS method is more cost efficient because minimal manipulation of the time domain data is involved. However, the PCD approach has another potential advantage unexplored in this paper: The SVD offers a practical way of filtering out any measurement noise or rigid-body mode contribution because these

are typically associated with singular values much smaller than those characteristic of the dynamics. This is a beneficial function of the PCD approach since time domain data is being used.

Several issues stem from the conclusion of this phase in the research. A significant one is how to efficiently generate more accurate response surfaces. One approach being considered as a possible answer to this issue is to incorporate the statistical software package, NESSUS, created by Southwest Research Institute [5], into the updating algorithm. This avenue would, at a minimum, allow for a more automated response surface generation process. It has the potential to considerably reduce the number of analyses that must be completed. Currently the interface between NESSUS and ABAQUS Explicit is still being developed. The use of the NESSUS/ABAQUS link will enable the efficient computation of response surfaces for many parameters with a relatively small number of runs. However, a more standard continuous-space optimization technique will be required because the complete space of model parameters will not have been exhaustively calculated. Typical problems with convergence, local vs. global minima, etc., will then need to be addressed. Also, applying the techniques to systems with more geometric complexity and limited instrumentation will lead to the classical issues involving test/analysis DOF mismatch.

Overall, the study described in this paper indicates that it should be possible to update constitutive model parameters for a nonlinear elastic polymer material using transient impact data. The next step will be the application of this technique to experimentally measured data. Finally, the techniques described will be applied to a large finite element model of a structure subjected to an explosive shock load.

Section 5. References

1. Maia, N.M.M., and Silva, J.M.M., **Theoretical and Experimental Modal Analysis**, Ed., Research Studies Press, Ltd., Wiley & Sons, New York, 1997.
2. Hasselman, T.K., Anderson, M.C., and Wenshui, G., "Principal Components Analysis For Nonlinear Model Correlation, Updating and Uncertainty Evaluation," *16th IMAC*, Santa Barbara, California, Feb. 2-5, 1998, pp. 664-651.
3. Mees, A.I., Rapp, P.E., and Jennings, L.S., "Singular Value Decomposition and Embedding Dimension," *Physical Review A*, Vol. 36, No. 1, July 1987, pp. 340-346.
4. **Instruction Manual for the Lansmont Model 610 Shock Test Machine**, Lansmont Corporation, Pacific Grove, CA,
5. **Abaqus/Explicit User's Manual**, Version 5.8, Hibbit, Karlsson & Sorensen, Inc., Pawtucket, RI, 1997.
6. **NESSUS User's Manual**, Version 2.3, Southwest Research Institute, San Antonio, TX, 1996